

# Reduction of Surface Roughness Induced Spin Relaxation in SOI MOSFETs

D. Osintsev, O. Baumgartner, Z. Stanojevic, V. Sverdlov, and S. Selberherr

Institute for Microelectronics, TU Wien, Guhausstrae 27–29/E360, 1040 Wien, Austria

E-mail: {sverdlov|baumgartner|stanojevic|osintsev|selberherr}@iue.tuwien.ac.at

**Abstract**—Silicon is the main element of modern charge-based electronics. Understanding the details of the spin propagation in silicon structures is elementary for novel spin-based device applications. We investigate valley splitting, surface roughness scattering, and spin relaxation matrix elements in thin silicon films by using a perturbative  $\mathbf{k} \cdot \mathbf{p}$  approach. We demonstrated that applying uniaxial stress along the [110] direction considerably suppresses the intersubband spin relaxation elements.

## I. INTRODUCTION

Electron spin properties in semiconductors are a subject of intensive studies due to their potential role in future spin-driven microelectronic devices [1], [2]. Utilizing the spin of electrons can provide a huge step for microelectronics to reduce power consumption and increase computational speed of various devices. The spin of an electron is quantized and possesses two different values. Thus, it makes spin incorporation in the currently binary logic possible. Silicon, the main material of microelectronics, is predominantly composed of nuclei with zero spin and is characterised by weak spin-orbit interaction. This ensures long distance spin propagation through the bulk [3], which in combination with a possibility of injecting spin at room temperature [4] or even elevated temperature [5] makes fabrication of spin-based switching devices in the near future plausible. However, the experimentally observed enhancement in spin relaxation in electrically gated lateral-channel silicon structures [6] is an obstacle in realizing spin-driven devices [7]. A deeper understanding of the fundamental spin relaxation mechanisms in silicon MOSFETs is urgently needed [8].

In this work we investigate the influence of the intrinsic spin-orbit interaction on the spin relaxation matrix elements due to surface roughness scattering in thin silicon films. Following [7], a  $\mathbf{k} \cdot \mathbf{p}$  approach [9], [10] suitable to describe the electronic subband structure in the presence of strain is generalized to include the spin degree of freedom. In contrast to [7], our effective  $4 \times 4$

Hamiltonian considers only the relevant [001] oriented valleys. With spin included the Hamiltonian describes the low-energy unprimed subband ladder. Without strain the unprimed subbands are degenerate. This degeneracy produces a large mixing of the spin-up and spin-down states, resulting in spin hot spots characterized by strong spin relaxation due to the spin-orbit coupling. Shear strain is able to efficiently lift the degeneracy between the unprimed subbands [10]. The energy splitting between the otherwise equivalent subbands removes the origin of the spin hot spots in a confined silicon system, which should substantially improve the spin lifetime in gated silicon systems.

## II. METHOD

We numerically investigated the dependences of the matrix elements responsible for surface roughness induced scattering and spin relaxation in silicon transistors as a function of shear strain and the quantum well width. For [001] oriented valleys in a (001) silicon film the Hamiltonian is written in the vicinity of the  $X$  point along the  $k_z$ -axis in the Brillouin zone. The basis is conveniently chosen as  $[(X_1, \uparrow), (X_1, \downarrow), (X_2, \uparrow), (X_2, \downarrow)]$ , where  $\uparrow$  and  $\downarrow$  indicate the spin projection at the quantization  $z$ -axis. In the Hamiltonian (2)  $m_t$  and  $m_l$  are the transversal and the longitudinal effective masses,  $k_0 = 0.15 \times 2\pi/a$  is the position of the valley minimum relative to the  $X$  point in unstrained silicon ( $a$  is the lattice constant),  $\varepsilon_{xy}$  denotes the shear strain component,  $M^{-1} \approx m_t^{-1} - m_0^{-1}$ , and  $D = 14\text{eV}$  is the shear strain deformation potential. The spin-orbit term  $\tau_y \otimes (k_x \sigma_x - k_y \sigma_y)$  with

$$\Delta_{\text{so}} = 2 \left| \sum \frac{\langle X_1 | p_j | n \rangle \langle n | [\nabla V \times \mathbf{p}]_j | X_2' \rangle}{E_n - E_X} \right|, \quad (1)$$

couples the states with opposite spin projections from the opposite valleys. Here  $\sigma_x$ ,  $\sigma_y$ , and  $\sigma_z$  are the spin Pauli matrices and  $\tau_y$  is the  $y$ -Pauli matrix in the valley degree of freedom.

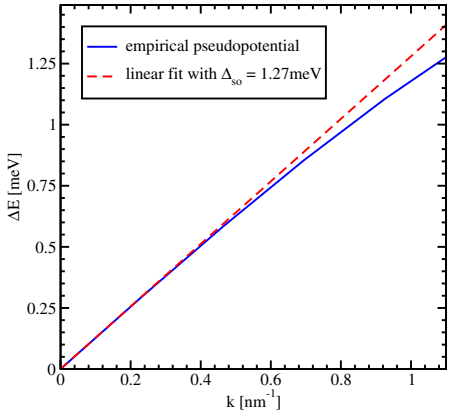


Fig. 1. Empirical pseudopotential calculations of the spin-orbit interaction strength by evaluating the gap opening at the  $X$ -point between  $X_1$  and  $X_2$  for finite  $k_x$ .

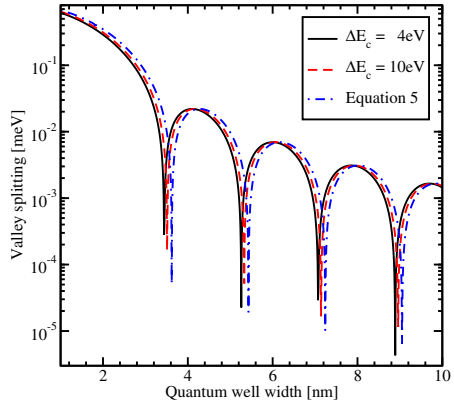


Fig. 2. Splitting of the lowest unprimed electron subbands as a function of the silicon film thickness for several values of the band offset at the interface. The shear strain value is 0.05%,  $k_x = 0.1\text{nm}^{-1}$ ,  $k_y = 0.1\text{nm}^{-1}$ .

with  $y_n$ ,  $\eta$ , and  $B$  defined as

$$H = \begin{bmatrix} H_1 & H_3 \\ H_3^\dagger & H_2 \end{bmatrix}, \quad (2)$$

where  $H_1$ ,  $H_2$ , and  $H_3$  are written as

$$H_j = \left[ \frac{\hbar^2 k_z^2}{2m_l} + \frac{(-1)^j k_0 k_z \hbar^2}{m_l} + \frac{(k_x^2 + k_y^2) \hbar^2}{2m_t} + U(z) \right] I, \quad (3)$$

$$H_3 = \begin{bmatrix} D\varepsilon_{xy} - \frac{k_x k_y \hbar^2}{M} & (k_y - k_x i) \Delta_{so} \\ (-k_y - k_x i) \Delta_{so} & D\varepsilon_{xy} - \frac{k_x k_y \hbar^2}{M} \end{bmatrix}. \quad (4)$$

Here  $j = 1, 2$ ,  $I$  is the identity  $2 \times 2$  matrix, and  $U(z)$  is the confinement potential. The value  $\Delta_{so} = 1.27\text{meV}\text{nm}$  computed by the empirical pseudopotential method (Figure 1) is close to the one reported in [7].

### III. RESULTS AND DISCUSSION

Splitting of the lowest unprimed electron subbands as a function of the silicon film thickness for several values of the conduction band offset at the interfaces is shown in Figure 2. The valley splitting oscillates with increasing film thickness. According to theory [11], the valley splitting of an infinite potential square well is given by

$$\Delta E_n = \frac{2y_n^2 B}{k_0 t \sqrt{(1 - y_n^2 - \eta^2)(1 - y_n^2)}} \times \left| \sin \left( \sqrt{\frac{1 - y_n^2 - \eta^2}{1 - y_n^2}} k_0 t \right) \right|, \quad (5)$$

$$y_n = \frac{\pi}{k_0 t}, \quad (6)$$

$$\eta = \frac{m_l B}{k_0^2 \hbar^2}, \quad (7)$$

$$B = \sqrt{\Delta_{so}^2 (k_x^2 + k_y^2) + \left( D\varepsilon_{xy} - \frac{\hbar^2 k_x k_y}{M} \right)^2}. \quad (8)$$

Here  $t$  is the film thickness. Because (5) is valid for an infinite potential square well, a slight deviation is observed between the theoretical curve and the numerically calculated curve for the conduction band offset value of 4eV in Figure 2. Large values of the conduction band offset show a better agreement of the analytically and the numerically obtained results.

The valley splitting as a function of the quantum well width for different values of the effective electric field is shown in Figure 3. Without electric field the valley splitting oscillates as in Figure 2. With electric field the oscillations are not observed in thicker films. According to Friesen *et al.* [12] the condition for the independence of the valley splitting from the quantum well width is

$$L^3 > \frac{2\pi^2 \hbar^2}{m_l e E_{field}}. \quad (9)$$

For thinner structures, the quantization is provided by the second barrier of the quantum well, and the shape of the oscillations is similar to that in the absence of an electric field. For an electric field of strength 0.05MV/cm the quantum well width should be larger than 6.9nm in order to observe the independence of the valley splitting on the quantum well width. This value is

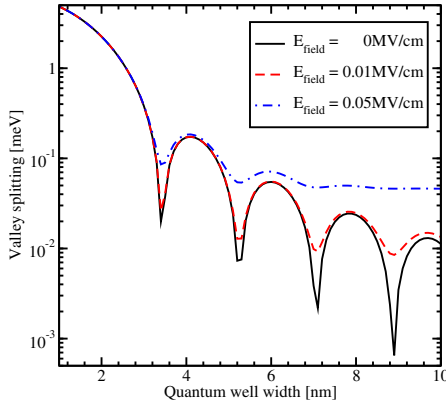


Fig. 3. Splitting of the lowest unprimed electron subbands as a function of the film thickness for different values of the effective electric field. The shear strain value is 0%, the conduction band offset is 4eV,  $k_x = 0.1\text{nm}^{-1}$ ,  $k_y = 0.1\text{nm}^{-1}$ .

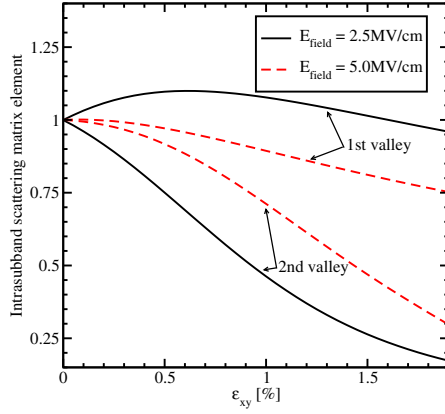


Fig. 4. Intra-valley scattering matrix elements normalized by their values for zero strain as function of shear strain for different electric fields.

in good agreement with the simulation results shown in Figure 3.

The surface roughness scattering matrix elements are taken to be proportional to the square of the product of the subband function derivatives at the interface [13]. A (001) silicon film of 4nm thickness is considered. The surface roughness at the two interfaces is assumed to be equal and statistically independent. It is described by a mean and a correlation length [13]. Figure 4 and Figure 5 show the dependences on strain and electric field of the matrix elements for intra-subband and inter-valley scattering. The intra-subband scattering matrix elements within both unprimed subbands show the tendency to decrease at higher shear strain values. Because the unprimed subbands are degenerate without applied shear strain, the elastic scattering inter-valley elements are zero. The degeneracy is lifted by applying shear

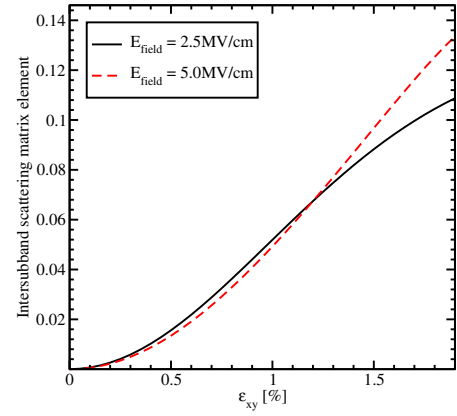


Fig. 5. Intervalley scattering matrix elements normalized to the value of the intravalley scattering at zero strain as a function of strain for different electric fields. Being elastic, this scattering is zero in unstrained samples, where the valleys are degenerate.

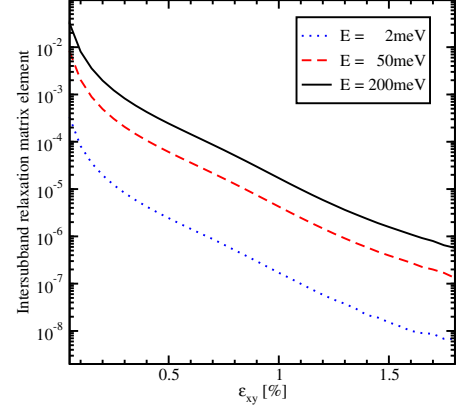


Fig. 6. Intervalley spin relaxation matrix elements normalized to intravalley scattering at zero strain dependence on shear strain for several values of the kinetic electron energy in the subband.

strain. This leads to non-zero inter-subband scattering elements. The increase of the inter-subband scattering elements with increasing shear strain is observed for different electric fields.

We now discuss the matrix elements mixing up- and down-spin states and their responsibility for the spin relaxation. The spin is injected along [001] direction. The mixing depends on the strength of the spin-orbit interaction as well as on the wave vectors  $k_x$ ,  $k_y$  and thus the kinetic energy within the subband. The dependence of the inter-valley spin relaxation matrix element mixing the up- and down-spin states from the two different subbands is shown in Figure 6 for the case, where the two wave vectors before and after collision are anti-parallel and aligned along the  $x$  axis. The spin relaxation value decreases rapidly with increasing strain due to the increased valley splitting. As soon as the valley splitting

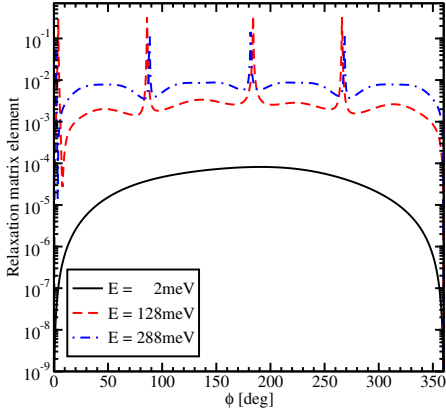


Fig. 7. Dependence of the normalized spin relaxation matrix elements on the angle between the incident and the relaxed wave for different values of the wave energy. The shear strain value is 0.1%.

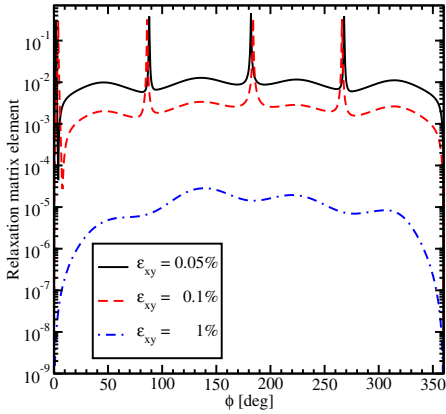


Fig. 8. Dependence of the normalized spin relaxation matrix elements on the angle between the incident and the relaxed wave for different values of strain. The wave energy value is 128meV.

becomes larger than the spin-orbit interaction strength characterized by  $\Delta_{\text{so}} \sqrt{k_x^2 + k_y^2}$ , the mixing of up- and down-spin states caused by this spin-orbit interaction is reduced.

The splitting of the valleys depends on  $D\varepsilon_{xy} - \hbar^2 k_x k_y / M$ , and their degeneracy is lifted by the kinetic-like term  $\hbar^2 k_x k_y / M$  even without shear strain. This results in a strong dependence of the surface roughness induced spin relaxation matrix elements on the angle between the incident and outgoing wave vectors. Figure 7 and Figure 8 show the dependences of the relaxation matrix elements on this angle for different values of shear strain and energy of the state. However, as follows from Figure 8, shear strain leads to the reduction of the spin relaxation matrix element in good agreement with Figure 6.

#### IV. CONCLUSION

We have investigated the lowest unprimed electron subband splitting in a SOI film for a wide range of parameters, including the film thickness, the shear strain, and the effective electric field value. We have included the spin-orbit interaction effects into the effective low-energy  $k \cdot p$  Hamiltonian to investigate the surface roughness induced spin relaxation. We have demonstrated that, due to the valley splitting increase, the matrix elements for the inter-valley spin relaxation decrease rapidly with shear strain. Thus, shear strain used to enhance electron mobility can also be used to boost spin lifetime.

#### ACKNOWLEDGMENT

This work is supported by the European Research Council through the grant #247056 MOSILSPIN.

#### REFERENCES

- [1] S. Sugahara and J. Nitta, "Spin-transistor electronics: an overview and outlook", Proceedings of the IEEE, vol. 98(12), pp. 2124–2154, 2010.
- [2] A. Makarov, V. Sverdlov, S. Selberherr, "Emerging memory technologies: trends, challenges, and modeling methods", Microelectronics Reliability, vol. 52(4), pp. 628–634, 2012.
- [3] B. Huang, D.J. Monsma, I. Appelbaum, "Coherent spin transport through a 350 Micron thick silicon wafer", Phys. Rev. Lett., vol. 99, pp. 177209, 2007.
- [4] S.P. Dash, S. Sharma, R.S. Patel, M.P. de Jong, R. Jansen, "Electrical creation of spin polarization in silicon at room temperature", Nature, vol. 462, pp. 491–494, 2009.
- [5] C.H. Li, O.M.J. Van't Erve, B.T. Jonker, "Electrical injection and detection of spin accumulation in silicon at 500K with magnetic metal/silicon dioxide contacts", Nat. Commun. vol. 2, pp. 245, 2011.
- [6] J. Li, I. Appelbaum, "Modeling spin transport in electrostatically-gated lateral-channel silicon devices: Role of interfacial spin relaxation", Phys. Rev. B, vol. 84, pp. 165318, 2011.
- [7] P. Li, H. Dery, "Spin-orbit symmetries of conduction electrons in silicon", Phys. Rev. Lett., vol. 107, pp. 107203, 2011.
- [8] Y. Song, H. Dery, "Analysis of phonon-induced spin relaxation processes in silicon", arXiv:1201.6660v1 [cond-mat.mtrl-sci] 2012.
- [9] G.L. Bir, G.E. Pikus, "Symmetry and strain-induced effects in semiconductors", New York/Toronto:J. Wiley & Sons, 1974.
- [10] V. Sverdlov, "Strain-induced effects in advanced MOSFETs", Springer, 2011.
- [11] V. Sverdlov, O. Baumgartner, T. Windbacher, and S. Selberherr, "Modeling of modern MOSFETs with strain", J. Comput. Electronics, vol. 8, pp. 3–4, 2009.
- [12] M. Friesen, S. Chutia, C. Tahan, S.N. Coppersmith, "Valley splitting theory of SiGe/Si/SiGe quantum wells", Phys. Rev. B, vol. 75, pp. 115318, 2007.
- [13] M.V. Fischetti, Z. Ren, P.M. Solomon, M. Yang, and K. Rim, "Six-band  $k \cdot p$  calculation of the hole mobility in silicon inversion layers: Dependence on surface orientation, strain, and silicon thickness", J. Appl. Phys., vol. 94, pp. 1079, 2003.